

**GRAPHENE-Fe<sub>3</sub>O<sub>4</sub>-TiO<sub>2</sub> TERNARY COMPOSITE: AN EFFICIENT  
VISIBLE LIGHT CATALYST FOR THE REMOVAL OF ORGANIC  
POLLUTANTS**

A

Dissertation

Submitted for the partial fulfilment for the

Degree of

Master of Science in Chemistry

Submitted by

**Swayam Prakash**

**&**

**Supriya Mishra**

**Roll no: 412CY2003**

**412CY2014**



**National Institute of Technology, Rourkela**

Under the guidance of

**Prof. Sasmita Mohapatra**

Assistant Professor  
Department of chemistry  
Rourkela, Odisha, India.  
Pin: 769008

## **ACKNOWLEDGEMENT**

We owe our cordial gratitude to my respected teacher and supervisor Dr. Sasmita Mohapatra, Assistant Professor, Department of Chemistry, National Institute of Technology, Rourkela, whose splendid guidance, authentic supervision, assiduous cooperation, moral support and constant encouragement enabled me to make out our research problem in the present form.

It is our great pleasure to acknowledge to Prof. N.Panda, Head of the Chemistry Department, National Institute of Technology, Rourkela for providing us the necessary facilities for making this research work a success.

We are highly indebted to all our teachers of this department for their kind help and expert suggestions. We express our profound gratitude to Ms. Swagatika Sahu, Mr. Smruti Ranjan Rout, Mr. Rahul Kumar Das and Mr. Subhajyoti Samanta for their ceaseless encouragement, immense help and hearty encouragement during our project work.

We wish to thank all of friends for making our stay in this institute a memorable experience. Finally, we are honestly grateful to our family members for their endless love, unending support & blessings & GOD who has always been a source of our strength, inspiration and our achievements.

Dr. Sasmita Mohapatra  
Assistant Professor,  
Department of Chemistry  
National Institute of Technology  
Rourkela  
Odisha-769008



---

## CERTIFICATE

This is to certify that the dissertation entitled, “**Graphene-Fe<sub>3</sub>O<sub>4</sub>-TiO<sub>2</sub> ternary composite: an efficient visible light catalyst for the removal of organic pollutants**” submitted by Mr. Swayam Prakash & Ms. Supriya Mishra for the award of Master of Science in Chemistry during the period of August 2013 - May 2014 in the Material Chemistry Laboratory, Department of Chemistry, National Institute of Technology, Rourkela, is a record of authentic work carried out by them under my supervision. To the best of my knowledge, the matter embodied in this dissertation has not been previously submitted for any degree in this/any other institute.

Date:

Dr. Sasmita Mohapatra

## **ABSTRACT**

A facile synthesis technique was employed for producing magnetic graphene-TiO<sub>2</sub> photocatalyst (GO-Fe<sub>3</sub>O<sub>4</sub>-TiO<sub>2</sub>). The synthesis method involves combination of sol-gel and assembling processes. The magnetic composite was characterized by, XRD, SEM, FESEM and UV-DRS analysis. The as synthesized material showed higher photocatalytic activity towards methylene blue (MB) degradation as compared with that of pure TiO<sub>2</sub> and GO-Fe<sub>3</sub>O<sub>4</sub> nanocomposite. Magnetic property of the nanocomposite defines it to be easily separable for repeated applications. These attractive physical properties and efficient photocatalytic activity quote GO-Fe<sub>3</sub>O<sub>4</sub>-TiO<sub>2</sub> nanocomposite as a promising photocatalyst under sunlight for practical use in wastewater treatment to control water pollution.

**Keywords:** Photocatalyst, Nanocomposite, Graphene oxide, Titanium dioxide, Iron oxide, Methylene blue.

## **CONTENTS**

	<b>Page</b>
<b>1. Introduction</b>	<b>1-2</b>
<b>2. A brief review of previous work</b>	<b>2-5</b>
<b>3. Objective of the present work</b>	<b>5</b>
<b>4. Experimental</b>	<b>6-7</b>
<b>5. Results and discussion</b>	<b>7-12</b>
<b>6. Conclusion</b>	<b>12</b>
<b>7. References</b>	<b>13-14</b>

## 1. INTRODUCTION:

The present scenario of water pollution management requires major attention for the future welfare of our civilization. It is estimated that around 10–15% of organic dyes are discharged in various ways in to the environment which has vary adverse effect on public health as well as on aquatic life.<sup>1</sup> Several conventional technologies such as membrane filtration, liquid-liquid extraction adsorption have been used to separate organic dye from water.<sup>2-4</sup> But these process have several demerits such as low adsorption capacity, non-recyclability, and complex operations for recycling.<sup>5,6</sup> Photo-catalysis is an advanced oxidation process (AOP) and has been considered as an effectively green, and low-cost method to degrade dyes.<sup>7-12</sup> Notably, titanium dioxide, a wide band-gap semiconductor with the capability of producing reactive oxygen species in water under UV radiation has proved effective for degrading organic materials, producing benign CO<sub>2</sub> as an end product.<sup>13</sup> This ability to remove contaminants completely and efficiently combined with low cost, low toxicity, and high abundance make it an ideal treatment platform for dealing with organic pollutants.<sup>14,15</sup> However, despite the existence of commercial TiO<sub>2</sub> formulations with excellent photocatalytic efficiency, they have found minimal use in industrial or commercial water treatment. One of the principal reasons for this is the difficulty associated with recovering nano-scale dispersions of the catalyst for re-use, diminishing the potential efficiency of the catalyst and posing an environmental threat due to the release of the catalyst to natural bodies of water.<sup>16,17</sup> Another serious issue is the need of ultraviolet (UV) light for activating the photocatalysts which greatly limits the technology in practical applications because of the low content of UV light in the solar spectrum (of about 2–3%).<sup>18-23</sup> As a result, research efforts have been made at exploiting new easily recoverable photocatalysts, which are photocatalytically active under visible light irradiation.

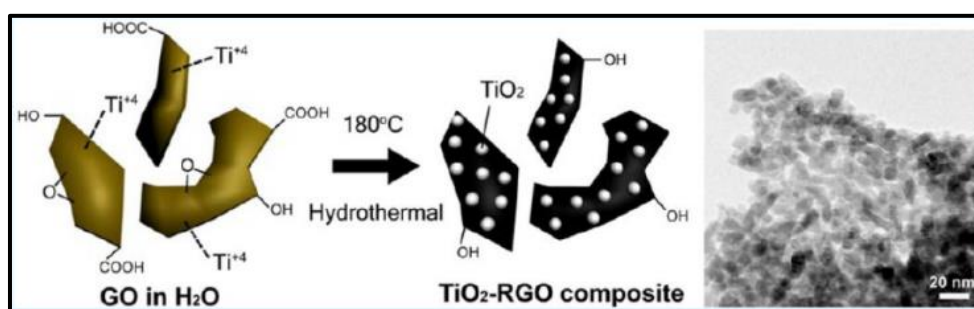
To address the recovery of TiO<sub>2</sub> catalyst, various techniques have been investigated including immobilization of TiO<sub>2</sub> nanomaterials on various substrates such as sand, glass or polymer beads, membranes, or magnetic nanoparticles.<sup>24-27</sup> While these techniques solve the problems associated with TiO<sub>2</sub> separation after treatment, they simultaneously introduce other problems related to photocatalytic efficiency, such as limiting dispersion of the catalyst throughout the solution thereby limiting interaction with contaminants.<sup>28</sup> This can be solved by investigating nanostructured support materials, such as magnetic nanoparticles or graphene oxide (GO) which has been the subject of recent research and

retain the ability to effectively disperse in solution. Graphene oxide (GO), a two-dimensional carbon material with unique mechanic and electronic properties, offers a good opportunity to prepare composite materials for photocatalysis applications. The band gap of GO can be tunable by just varying the oxidation level. The electronic properties of GO have been reported to provide enhancement of TiO<sub>2</sub> photocatalysis by reducing carrier recombination and increasing light absorption range, giving significant advantages to using GO as support structures.<sup>28-32</sup> Recyclability of such TiO<sub>2</sub> nanocomposites has also been enhanced by depositing magnetic nanoparticles on the same platform.

## 2. BRIEF REVIEW ON SYNTHESIS OF GRAPHENE OXIDE BASED PHOTOCATALYST

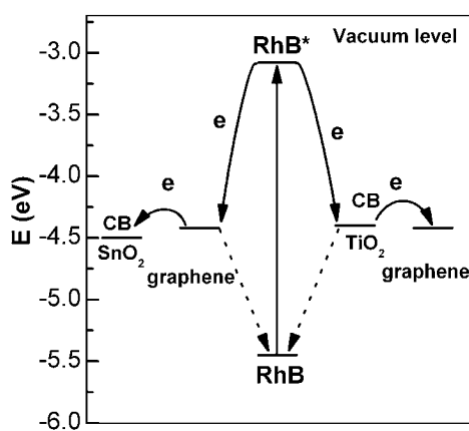
Owing to the challenging task for synthesis of highly efficient GO based photocatalyst, this review focuses on various current synthetic strategies used to produce GO-TiO<sub>2</sub> based photocatalyst. The knowledge of this review offers us valuable insight and inspiration to synthesize an efficient recyclable graphene oxide based visible catalyst.

Various methods have been reported on synthesis of GO-TiO<sub>2</sub> based photocatalyst including sol-gel deposition techniques, electrostatic attraction, and thermal or hydrothermal reduction. Typically, these synthetic techniques involve reaction of precursors to form TiO<sub>2</sub> directly on the surface of the GO support. A series of TiO<sub>2</sub>-reduced graphene oxide (RGO) nanocomposites were prepared by simple one-step hydrothermal reactions using the titania precursor, TiCl<sub>4</sub> and graphene oxide (GO) without reducing agents.<sup>33</sup> Hydrolysis of TiCl<sub>4</sub> and mild reduction of GO were simultaneously carried out under hydrothermal conditions. In addition, the photocatalytic activities of the synthesized composites were measured for the degradation of rhodamine B dye. The catalyst also can degrade a colorless dye such as benzoic acid under visible light. It showed enhanced catalytic activity compared to conventional TiO<sub>2</sub> photocatalyst, P25.



Scheme 1: Schematic illustration of synthesis of TiO<sub>2</sub>-RGO composite<sup>33</sup>

Xu et al. reported a TiO<sub>2</sub>-Graphene nanocomposite for gas-phase photocatalytic degradation of volatile aromatic pollutant. The nanocomposite was prepared via a facile hydrothermal reaction of graphene oxide and TiO<sub>2</sub> in an ethanol-water solvent. By investigating the effect of different addition ratios of grapheme on the photocatalytic activity of TiO<sub>2</sub>-GR systematically, they found that the higher weight ratio in TiO<sub>2</sub>-GR decrease the photocatalytic activity.<sup>34</sup> Graphene-metal-oxide composites were reported by Zhao and his co-workers for the degradation of dyes under visible light irradiation.<sup>35</sup> Reduced grapheme oxide (RGO) was respectively modified with tin dioxide (SnO<sub>2</sub>) and titanium dioxide (TiO<sub>2</sub>) via a direct redox reaction between the graphene oxide (GO) and the reactive cations Sn<sup>2+</sup> and Ti<sup>3+</sup>, forming RGO-SnO<sub>2</sub> and RGO-TiO<sub>2</sub> composites. During this redox reaction, GO was reduced to RGO while Sn<sup>2+</sup> and Ti<sup>3+</sup> were oxidized to SnO<sub>2</sub> and TiO<sub>2</sub>, depositing on the surface of the RGO. The composite materials were found to exhibit very interesting photocatalytic properties for degrading Rhodamine B under visible light irradiation.

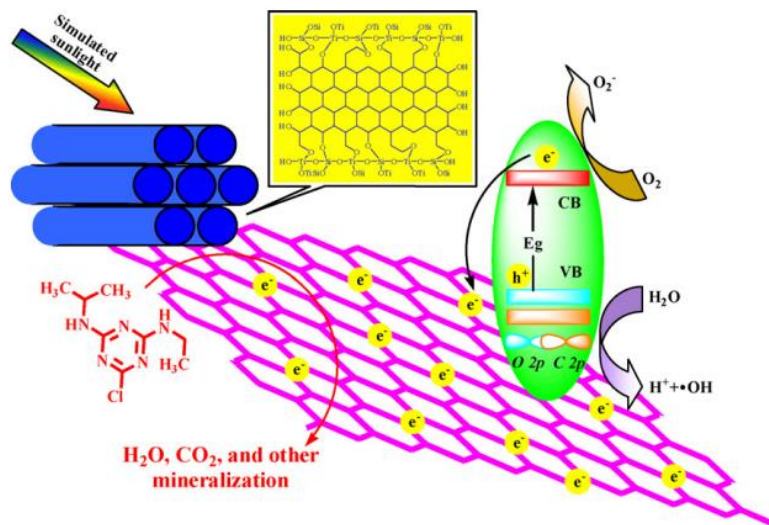


Scheme-2: The energy diagrams of RhB, graphene, TiO<sub>2</sub> and SnO<sub>2</sub><sup>35</sup>

Ordered mesoporous graphene-titania/silica composites with an anatase phase structure were prepared by Yan et al. using a direct sol-gel co-condensation technique combined with hydrothermal treatment in the presence of the triblock copolymer non-ionic surfactant P123.<sup>36</sup> The textural properties of the as-prepared composites were controlled by changing grapheme loading and titania-to-silica molar ratio. These composites were applied to the degradation of the aqueous endocrine-disrupting chemical atrazine under simulated sunlight irradiation. The

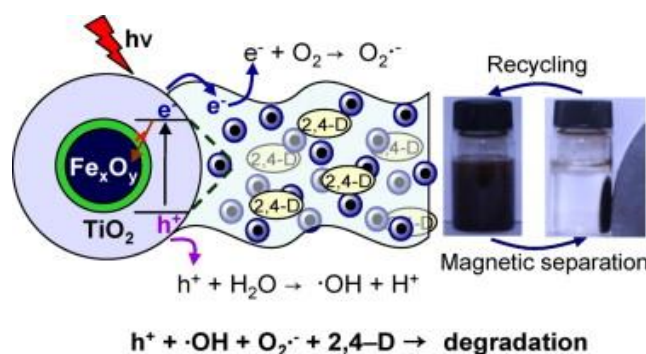


reasons for the enhanced photocatalytic activity of the single or co-doped photocatalyst were also revealed by them.



Scheme 3: Textural properties and electronic structures of ordered mesoporous graphene–TiO<sub>2</sub>/SiO<sub>2</sub> composite.<sup>36</sup>

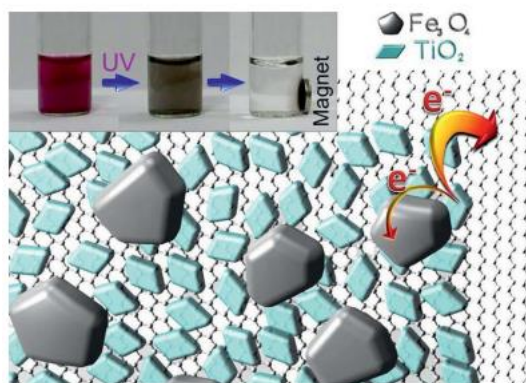
Recently, Tang et al. have produced a magnetically separable nanocomposite consisting of silica insulated Fe<sub>3</sub>O<sub>4</sub> particles coated in TiO<sub>2</sub> anchored to a reduced GO sheet.<sup>37</sup> The catalyst exhibited strong light absorption in the visible region and high adsorption capacity to organic pollutants, resulting in almost 100% photocatalytic removal efficiency of typical herbicide 2,4-dichlorophenoxyacetic acid from water under simulated solar light irradiation, far higher than 33% on commercial P25. This formulation imparted both magnetic separation capability and superior light harvesting to the photocatalyst.



Scheme 4: Mechanistic pathway for herbicide degradation<sup>37</sup>

In a similar study, Lin et al. deposited Fe<sub>3</sub>O<sub>4</sub> nanoparticles and TiO<sub>2</sub> nanoparticles on rGO to achieve improved separability and light capture over native TiO<sub>2</sub>.<sup>38</sup> Additionally, they

postulated that the rGO support helped mitigate photodissolution that would otherwise occur between  $\text{TiO}_2$  and  $\text{Fe}_3\text{O}_4$  by acting as an electron sink, preventing oxidation of the iron oxide.



Scheme 5: Schematic illustration of the structure and electron transfer in GTF<sup>38</sup>

A modular synthesis technique was developed for producing graphene-supported titanium dioxide photocatalysts.<sup>39</sup> The modular synthesis allowed for simple tuning of the ratio of particle loading on the graphene oxide (GO) surface as well as good photocatalytic activity of the composite and quick, efficient magnetic separability. GO flakes were used as a support for titanium dioxide nanoparticles and  $\text{SiO}_2$  insulated nano-sized magnetite aggregates. The synthesised photocatalyst shows excellent activity for degradation of methylene blue under UV irradiation. Above three examples demonstrated the capability of the nanocomposite to be recovered and re-used in subsequent trials.

### 3. OBJECTIVE OF THE PRESENT WORK

Recently, much attention has been focused on fabrication of recyclable photocatalyst for organic pollutant removal. Therefore, development of highly dispersible efficient visible light photocatalyst by an easy method involving cheap and easily available starting materials is desirable. In this regard, our present investigation is addressed on the followings

- Synthesis of magnetic  $\text{GO-Fe}_3\text{O}_4\text{-TiO}_2$  photocatalyst.
- Characterization of the phase, morphology, electronic properties, zeta potential using standard characterization techniques like X-ray diffraction technique, Scanning electron microscope (SEM), UV-visible-DRS etc.
- Investigation on catalytic efficiency  $\text{GO-Fe}_3\text{O}_4\text{-TiO}_2$  in photocatalytic degradation of organic pollutants under sunlight.

## **4. EXPERIMENTAL**

### **4.1. Materials And Method**

Graphite powder, sulphuric acid and hydrogen peroxide was procured from SDFine Chemicals, India. Titanium isopropoxide was supplied by Spectrochem, India.  $\text{NaNO}_3$ ,  $\text{KMnO}_4$ ,  $\text{FeCl}_3$ ,  $\text{FeSO}_4$ ,  $\text{CH}_3\text{COONa}$ , ethylene glycol, ethanol amine were purchased from Merck India and all chemicals were used as supplied without further purification. Millipore water (18.2 M $\Omega$  cm) was used throughout the experiment.

### **4.2. Synthesis of Graphene- $\text{Fe}_3\text{O}_4$ - $\text{TiO}_2$ ternary photocatalyst**

#### **4.2.1. Preparation of Graphene Oxide (GO)**

GO was prepared from purified natural graphite powder according to the Hummers method. In detail, graphite powder (1.0 g),  $\text{NaNO}_3$  (0.5 g) and  $\text{KMnO}_4$  (3.0 g) were slowly added to a concentrated  $\text{H}_2\text{SO}_4$  solution (23 ml) within an ice bath. After removing the ice bath, the above mixture was intensely stirred at 35 °C for 30 min. After the reaction was completed, deionized water (46 ml) was added to above mixture while keeping the temperature at 98 °C for 15 min, followed by reducing the temperature to 60 °C with the addition of warm deionized water (140 ml) and  $\text{H}_2\text{O}_2$  (30%, 10 ml) with continuous stirring for 2 h. The obtained mixture was centrifuged to collect the solid product and washed with 4wt% HCl solution 5 times and then with deionized water until the pH of the supernatant was neutral. Finally the material was dried to obtain a loose brown powder.

#### **4.2.2. Synthesis of $\text{Fe}_3\text{O}_4$**

Amine functionalised magnetic  $\text{Fe}_3\text{O}_4$  nanoparticles were prepared by thermal decomposition of  $\text{FeSO}_4$  and  $\text{FeCl}_3$  in ethylene glycol in presence of sodium acetate and ethanolamine. Briefly, anhydrous  $\text{FeCl}_3$  (683 mg, 4.2 mmol) and  $\text{FeSO}_4$  (584 mg, 2.1 mmol) were taken in 30 ml ethylene glycol and 0.5 g of sodium acetate was added to it. The black colour solution thus obtained was stirred for 30 min at 80 °C followed by the addition of 15 ml of ethanolamine. The entire solution was heated at 150 °C for 6 h during which fine black colloidal particles appeared in the reaction mixture. Then it was cooled down to room temperature. The particles were recovered using a magnetic separator, washed with milipore water and re-dispersed in milipore water for further use.

#### **4.2.3. Synthesis of GO- $\text{Fe}_3\text{O}_4$ - $\text{TiO}_2$ nanocomposite**

The prepared graphene oxide (GO) was dispersed in water to form a homogeneous solution with concentration of 0.5mg/ml. 4 ml portion of  $\text{Fe}_3\text{O}_4$  suspension (5mg/ml) was mixed with

40 ml of GO solution and stirred for 2 h at room temperature. After magnetic separation, 5mg of intermediate Fe<sub>3</sub>O<sub>4</sub>-GO was dispersed in alcohol/water (140ml/10ml) mixture and heated to 70 °C. Then, 360µl Ti(iPr)<sub>4</sub> and 150µl H<sub>2</sub>SO<sub>4</sub> were added and the solution was mechanically stirred for 12h at the same temperature. The prepared GO-Fe<sub>3</sub>O<sub>4</sub>-TiO<sub>2</sub> nanocomposite was magnetically separated and washed with ethanol followed by water. The catalyst was oven dried at 70 °C for 6 h.

#### 4.3. Photocatalytic degradation of methylene blue (MB)

Photocatalytic degradation of methylene blue (MB) was conducted under sunlight using a batch technique. An accurately weighed quantity of GO-Fe<sub>3</sub>O<sub>4</sub>-TiO<sub>2</sub> (10 mg) was added to 20 ml of stirred 20 ppm MB solution taken in flat-bottom flask equipped with a magnetic stirrer. At specific time intervals, aliquots of suspension were collected, magnetically separated and used for determination of dye concentration using UV-vis spectrometer at characteristic wavelengths (MB, λ<sub>max</sub> 660 nm)

Residual content of the MB is calculated by the following formula:

$$\text{Residual content (n)\%} = \frac{C_t}{C_0} \times 100$$

in which C<sub>t</sub> is MB concentration at time “t”, and C<sub>0</sub> is the initial concentration of the MB under study. The effects of catalyst dose, time on degradation were studied.

#### 4.4. Characterization

The crystalline phase of the synthesised nanocomposite was investigated by an Expert Pro Phillips X-ray diffractometer. UV-DRS spectra were obtained using a Shimadzu 220V (E) UV-vis spectrophotometer. The morphology and microstructure were analysed by scanning electron microscope (HITACHI COM-S-4200) operated at 300 kV.

### 5. RESULTS AND DISCUSSION

The as-synthesized Fe<sub>3</sub>O<sub>4</sub> nanoparticles were first assembled by electrostatic interaction on the surface of graphene oxide (GO), which was prepared according to a modified Hummer's method. Then, TiO<sub>2</sub> was introduced by in situ growth from the precursor titanium isopropoxide in a mixture of alcohol and water which results in the formation of GO-Fe<sub>3</sub>O<sub>4</sub>-TiO<sub>2</sub> nanocomposite. In this case, pristine graphene nanosheets were bifunctionalized by Fe<sub>3</sub>O<sub>4</sub> and TiO<sub>2</sub> nanoparticles, which acted as targets for magnetic separation and photocatalytic activity.

Fig. 1 shows the XRD patterns of samples GO, GO-Fe<sub>3</sub>O<sub>4</sub>, GO-Fe<sub>3</sub>O<sub>4</sub>-TiO<sub>2</sub>. For the sample GO, the sharp peak at about  $2\theta = 10.4^\circ$  corresponds to the (002) reflection of stacked GO sheets with an interlayer spacing of 0.86 nm, larger than that of pristine graphite (0.34 nm).<sup>35</sup> This suggests the introduction of oxygen-containing groups on the GO sheets. For sample of GO-Fe<sub>3</sub>O<sub>4</sub> no diffraction peaks of layered GO can be seen, indicating the absence of layer-stacking regularity after deposition of Fe<sub>3</sub>O<sub>4</sub>. The XRD peaks at about  $2\theta = 30.2^\circ$ ,  $35.7^\circ$ ,  $43.3^\circ$ ,  $53.6^\circ$ ,  $57.4^\circ$ ,  $62.9^\circ$  can be indexed to the diffractions of Fe<sub>3</sub>O<sub>4</sub> (220), (311), (400), (511) and (440) planes (JCPDS, no. 01-1111). In final composite the appearance of additional reflection peaks at  $2\theta = 25.1^\circ$ ,  $38.0^\circ$ ,  $47.7^\circ$ ,  $53.9^\circ$  correspond to (101), (103), (200) and (105) crystal planes of anatase TiO<sub>2</sub> (JCPDS, no. 01-0562) confirms the successful growth of TiO<sub>2</sub> on GO-Fe<sub>3</sub>O<sub>4</sub> nanocomposite.

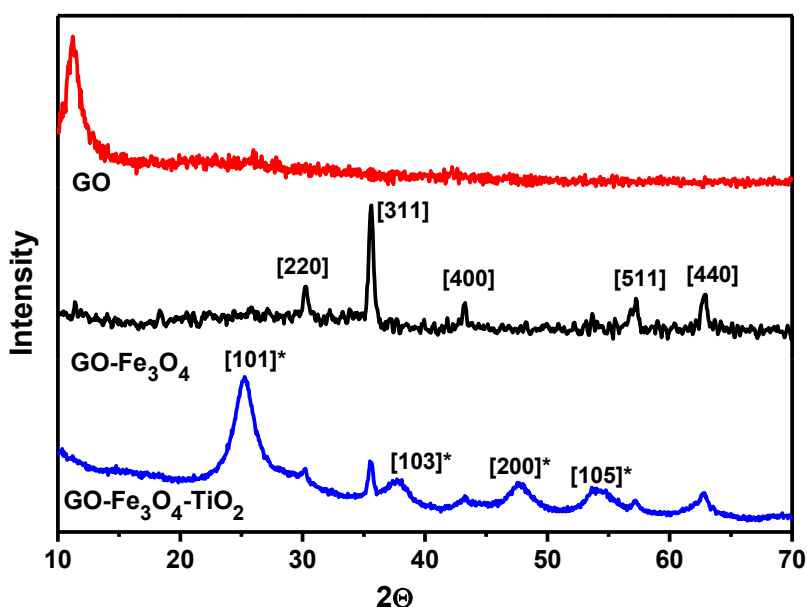


Fig. 1 XRD pattern of GO, GO-Fe<sub>3</sub>O<sub>4</sub> and GO-Fe<sub>3</sub>O<sub>4</sub>-TiO<sub>2</sub> (\* indicates the plane of TiO<sub>2</sub>)

The morphology of ternary composite was investigated through SEM and FESEM technique. The SEM image (Fig. 2a) clearly show that many particles in inhomogeneous size were deposited on the sheets of GO. The layered structure of GO is clearly distinguished in FESEM image (Fig. 2 b,c). High loading concentration of Fe<sub>3</sub>O<sub>4</sub> gave severe aggregation of the Fe<sub>3</sub>O<sub>4</sub>-TiO<sub>2</sub> nanoparticles and uneven dispersion across the GO surface. The EDS (Fig. 2 d) results further confirm the existence of Ti and Fe elements on GO sheets. The appearance of Si element is due to sample preparation on glass slide for SEM analysis.

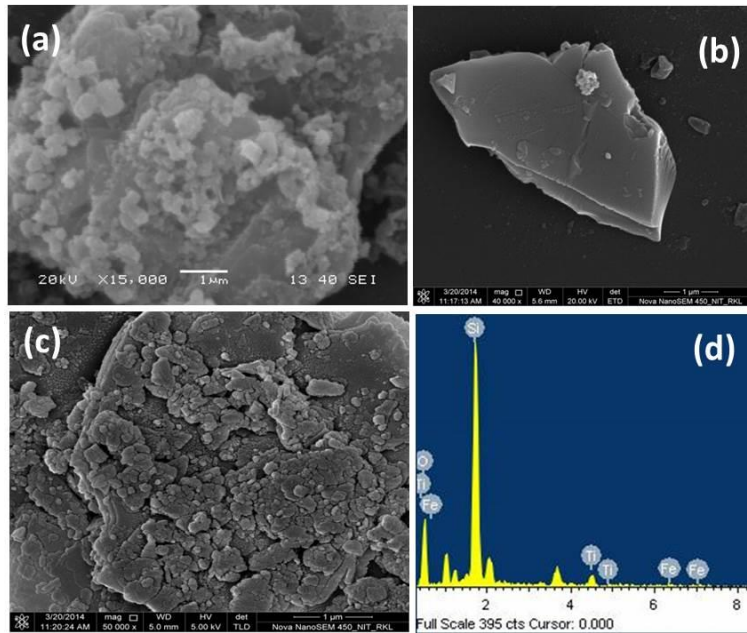


Fig. 2 SEM image (a), FESEM image (b), magnified FESEM image (c) and EDS spectrum (d) of GO-Fe<sub>3</sub>O<sub>4</sub>-TiO<sub>2</sub>,

The band gap of the nanocomposite was measured by using the following equation derived by Tauc and Devis Mott independently:

$$\alpha h\nu = K (h\nu - E_g)^n$$

where  $\alpha$  was the absorption coefficient,  $h\nu$  was the energy of the incident light,  $E_g$  was the optical energy gap or the band gap and  $n$  was a number which characterized the optical absorption processes. For direct transition  $n=1/2$  and for indirect transition  $n=2$ . For high absorbing region, where  $\alpha$  obeyed the above equation, by plotting  $(\alpha h\nu)^2$  as a function of photon energy ( $h\nu$ ) (Fig. 3) and extrapolating the linear regions of this curve to  $(\alpha h\nu)^2 = 0$ , the value of  $E_g$  was obtained as 1.5 eV which was direct band gap of the material which is lower than TiO<sub>2</sub> (3.2 eV)<sup>33</sup> and GO-TiO<sub>2</sub> composite (2.8 eV).<sup>40</sup> Such tuned band gap of the synthesised nanocomposite is suitable for exhibiting high photocatalytic activity.

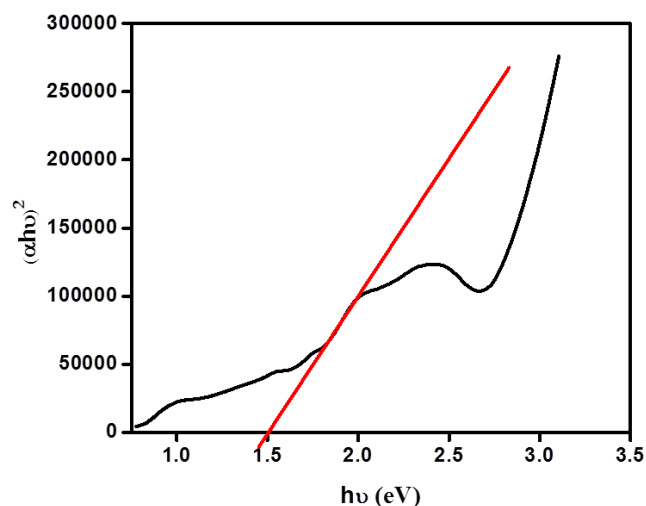


Fig. 3 Determination of band gap energy of GO-Fe<sub>3</sub>O<sub>4</sub>-TiO<sub>2</sub>

After synthesis of the nanocomposite, dye degradation experiments were carried out to assess the photocatalytic efficiency taking methylene blue as a model dye. The effect of increasing catalyst loading while maintaining a constant MB concentration is shown in Fig. 4. As expected, the amount of MB degradation increases with increased catalyst concentration. Increase in degradation with increase in loading capacity of catalyst is due to availability of greater number of active sites on the surface for adsorption of dye and subsequent photocatalytic degradation.

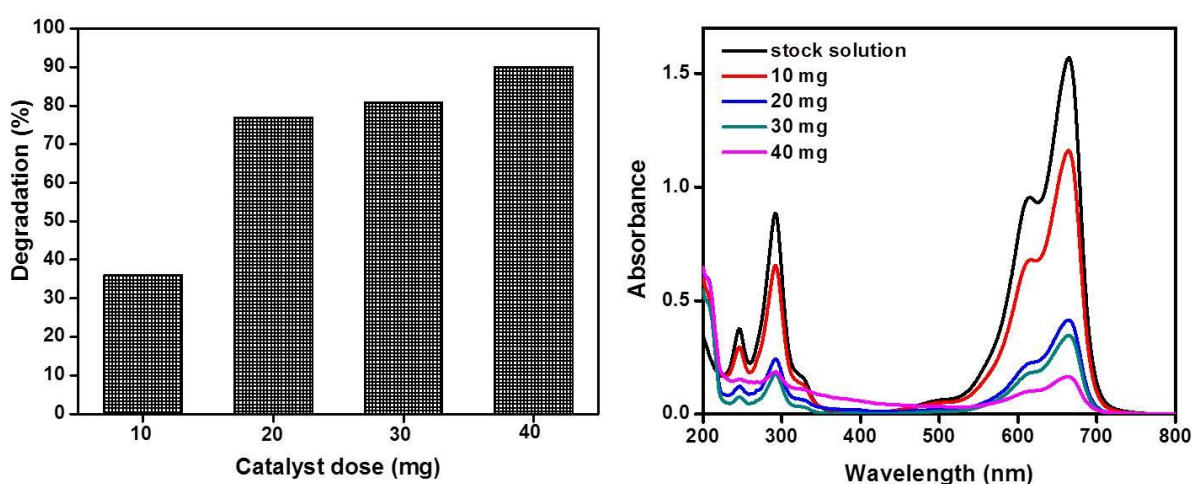


Fig. 4 Degradation of MB as a function of catalyst GO-Fe<sub>3</sub>O<sub>4</sub>-TiO<sub>2</sub> dose (MB 20 ppm, 20 ml, time 10 min)

To optimise the photocatalytic degradation time, the experiment was carried out for different time interval (Fig. 5). The catalyst shows almost 96% degradation at 10 min which reaches to

100% after 20 min. The synthesised ternary composite shows high photocatalytic activity and requires only 10 min for efficient degradation of MB.

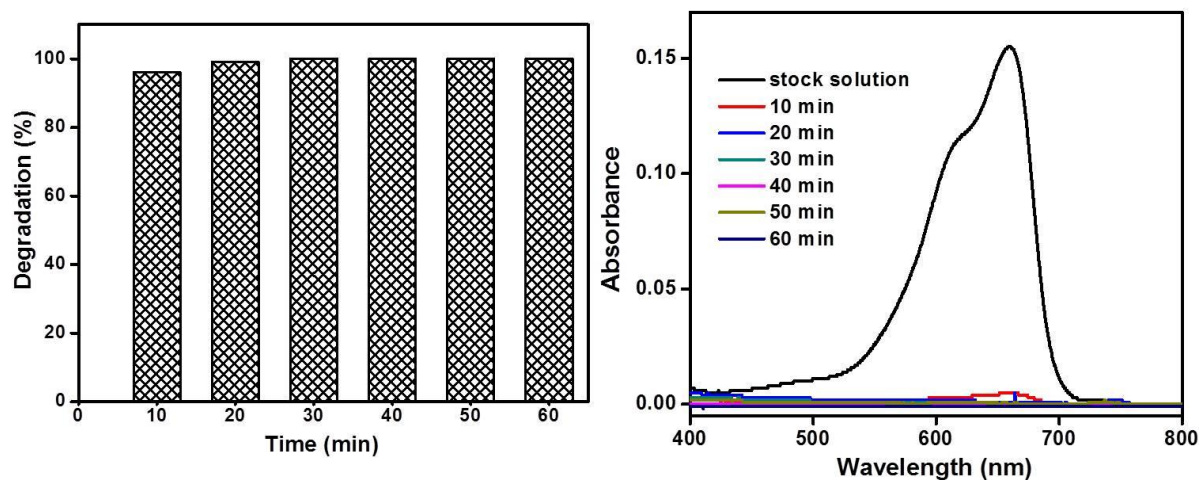


Fig. 5 Effect of time on MB degradation (MB 20 ppm, 20 ml, GO-Fe<sub>3</sub>O<sub>4</sub>-TiO<sub>2</sub> 10 mg)

We compared the photocatalytic activities of Fe<sub>3</sub>O<sub>4</sub>, GO-TiO<sub>2</sub> and GO-Fe<sub>3</sub>O<sub>4</sub>-TiO<sub>2</sub> nanocomposite in the degradation of MB by irradiation with sunlight (Fig. 6). The degradation rate of MB in contact with ternary nanocomposite GO-Fe<sub>3</sub>O<sub>4</sub>-TiO<sub>2</sub> shows highest activity. This improvement can be attributed to electrostatic interactions between GO and TiO<sub>2</sub> lengthening the carrier lifetime and favorable adsorption of methylene blue to the GO surface through  $\pi$ - $\pi$  stacking interactions as reported in previous works.<sup>39</sup> The effect of magnetic particle (Fe<sub>3</sub>O<sub>4</sub>) loading on separation efficiency of the nanocomposite was clearly shown by the Fig. 7 which demonstrates that easy separation of the catalyst through external magnet.

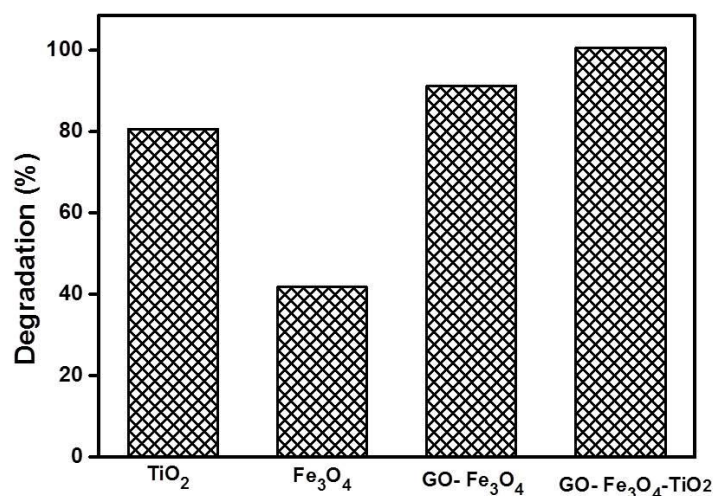


Fig. 6 Comparative study of MB degradation with TiO<sub>2</sub>, Fe<sub>3</sub>O<sub>4</sub>, GO-Fe<sub>3</sub>O<sub>4</sub> and Go-Fe<sub>3</sub>O<sub>4</sub>-TiO<sub>2</sub> (MB 20 ppm, 20 ml, catalyst 10 mg, time 10 min)



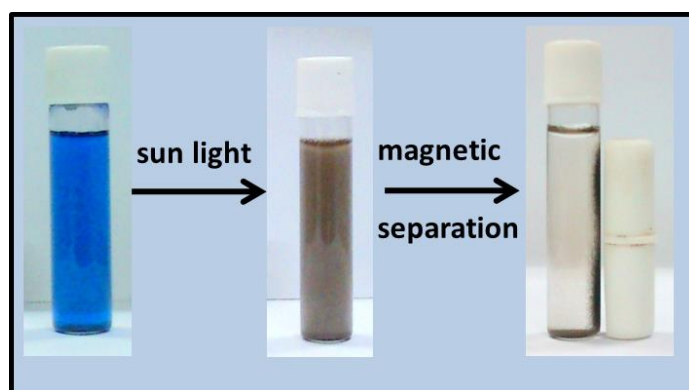


Fig. 7 Digital photograph of magnetic separation

The photocatalytic activities of the GO-Fe<sub>3</sub>O<sub>4</sub>-TiO<sub>2</sub> might be explained as follows (Fig. 8).<sup>37</sup> Upon light irradiation, TiO<sub>2</sub> nanoparticles undergo charge separation to yield electrons (e<sup>-</sup>) and holes (h<sup>+</sup>). Because graphene sheets are known as good electron acceptors, the electrons are quickly transferred to the graphene sheets. The negatively charged graphene sheets can react with the dissolved oxygen to produce superoxide anion radicals which reacts with hydrogen ions to make hydroxyl radicals while the holes are scavenged by the adsorbed water to form hydroxyl radicals. Finally, the active species (holes, superoxide anion radicals, and hydroxyl radicals) oxidize the MB molecules adsorbed on these active sites of the GO-Fe<sub>3</sub>O<sub>4</sub>-TiO<sub>2</sub> system through  $\pi$ - $\pi$  stacking interactions and/or electrostatic interaction.

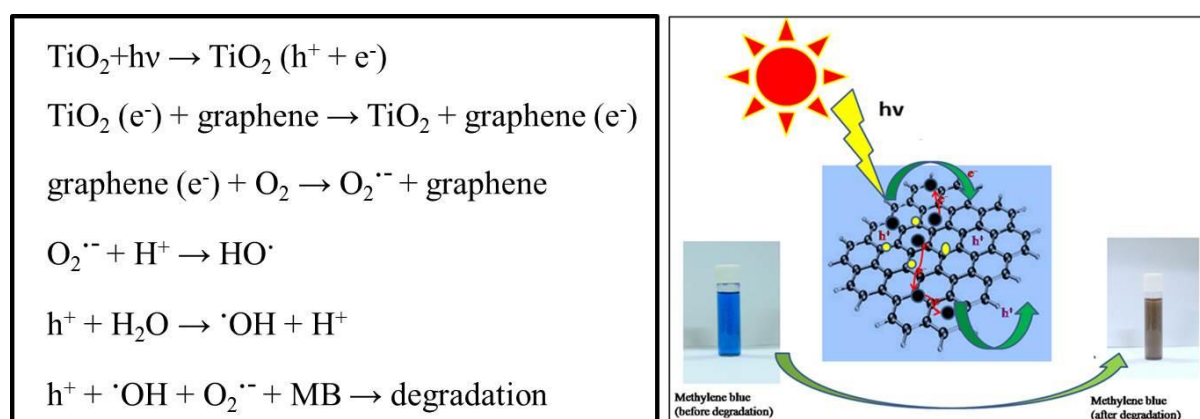


Fig. 8 Mechanistic pathway for MB degradation

## 6. CONCLUSION

A facile method was developed and explored for synthesis of highly photocatalytic active magnetically recyclable nanocomposite. This method allows for easily scalable production of the material, a factor critical to the implementation of nano-based water treatment techniques.

The formation of GO-Fe<sub>3</sub>O<sub>4</sub>-TiO<sub>2</sub> was confirmed by XRD. The narrow band gap of the synthesised nanocomposite sensitized the wide band gap of TiO<sub>2</sub> in the visible region, confirmed by UV-DRS. In addition, the synthesised photocatalyst exhibits high removal efficiency for MB under solar light, easy separation and good stability. These results suggest that the designed photocatalyst should be a general and competent platform for the removal of organic pollutants.

## REFERENCES

1. M. A. Al-Ghouti, M. A. M. Khraisheh, S. J. Allen, M. N. Ahmad, *J. Environ. Manage.* 2003, **69**, 229.
2. T. Zhang, L.L. Ding, H.Q. Ren, X. Xiong, *Water Res.* 2009, **43**, 5209.
3. J. Mansouri, S. Harrisson, V. Chen, *J. Mater.Chem.* 2010, **20**, 4567.
4. X.G. Li, R. Liu, M.R. Huang, *Chem. Mater.* 2005, **17**, 5411.
5. F. He, J. T. Fan, D. Ma, L. M. Zhang, C. Leung, H. L. Chan, *Carbon* 2010, **48**, 3139.
6. Z. G. Geng, Y. Lin, X. X. Yu, Q. H. Shen, L. Ma, Z. Y. Li, N. Pan, X. P. Wang, *J. Mater. Chem.* 2012, **22**, 3527.
7. A. Fujishima, X. T. Zhang, D. A. Tryk, *Surf. Sci. Rep.* 2008, **63**, 515.
8. P. V. Kamat, *Chem. Rev.* 1993, **93**, 267.
9. M. R. Hoffmann, S. T. Martin, W. Choi, D. W. Bahnemann, *Chem. Rev.* 1995, **95**, 69.
10. D. Ravelli, D. Dondi, M. Fagnoni, A. Albini, *Chem. Soc. Rev.* 2009, **38**, 1999.
11. J. Zeng, J. L. Huang, C. Liu, C. H. Wu, Y. Lin, X. P. Wang, S. Y. Zhang, J. G. Hou, Y. N. Xia, *Adv. Mater.* 2010, **22**, 1936.
12. B. Gao, Y. Lin, S. J. Wei, J. Zeng, Y. Liao, L. G. Chen, D. Gold-feld, X. P. Wang, Y. Luo, Z. C. Dong, J. G. Hou, *Nano Res.* 2012, **5**, 88.
13. J.M. Herrmann, *Appl. Catal. B* 2010, **99**, 461.
14. M. N. Chong, B. Jin, C.W.K. Chow, C. Saint, *Water Res.* 2010, **44**, 2997.
15. T. Leshuk, P. Everett, H. Krishnakumar, K. Wong, S. Linley, F. Gu, *J. Nanosci. Nanotechnol.* 2013, **13**, 3127.
16. Liu, S.-Q. *Environ. Chem. Lett.* 2011, **10**, 209.
17. Zhao, X. Lv, L. Pan, B. Zhang, W. Zhang, S. Zhang, *Q.Chem. Eng. J.* 2011, **170**, 381.
18. G. Liu, T. Wu, J. Zhao, H. Hidaka, N. Serpone, *Environ. Sci. Technol.* 1999, **33**, 2081.

19. M. R. Hoffmann, S. T. Martin, W. Choi, D. W. Bahnemann, *Chem. Rev.* 1995, **95**, 69.
20. M. A. Shannon, P. W. Bohn, M. Elimelech, J. G. Georgiadis, B. J. Marinas, A. M. Mayes, *Nature* 2008, **452**, 301.
21. S. Shanmugasundaram, K. Horst, *Angew. Chem., Int. Ed.* 2003, **42**, 4908.
22. S. Malato, P. Fernandez-Ibanez, M. I. Maldonado, J. Blanco, W. Gernjak, *Catal. Today* 2009, **147**, 1.
23. L. Zhao, X. Chen, X. Wang, Y. Zhang, W. Wei, Y. Sun, M. Antonietti, M. M. Titirici, *Adv. Mater.* 2010, **22**, 3317.
24. W. Qiu, Y. Zheng, *Appl. Catal. B* 2007, **71**, 151.
25. C. Shen, Y. J. Wang, J. H. Xu, G. S. Luo, *Chem. Eng. J.* 2012, **209**, 478.
26. H. Zhang, L. Yang, *Thin Solid Films* 2012, **520**, 5922.
27. S. Watson, J. Scott, D. Beydoun, R. J. Amal, *Nanopart. Res.* 2005, **7**, 691.
28. S. Malato, P. Fernández-Ibáñez, M. I. Maldonado, J. Blanco, W. Gernjak, *Catal. Today* 2009, **147**, 1.
29. K. S. Novoselov, *Science* 2004, **306**, 666.
30. C. Lee, X. Wei, J. W. Kysar, J. Hone, *Science* 2008, **321**, 385.
31. R. R. Nair, P. Blake, A. N. Grigorenko, K. S. Novoselov, T. J. Booth, T. Stauber, N. M. R. Peres, A. K. Geim, *Science* 2008, **320**, 1308.
32. L. X. Zhang, Y. Li, Y. Wang, J. Li, *ACS Nano* 2010, **4**, 380.
33. Md. S. A. S. Shah, A. R. Park, K. Zhang, J. H. Park, P. J. Yoo, *ACS Appl. Mater. Interfaces* 2012, **4**, 3893.
34. Y. Zhang, Z. R. Tang, X. Fu, Y. J. Xu, *ACS Nano* 2010, **4**, 7303.
35. J. Zhang, Z. Xiong, X. S. Zhao, *J. Mater. Chem.*, 2011, **21**, 3634.
36. K. Li, T. Chen, L. Yan, Y. Dai, Z. Huang, J. Xiong, D. Song, Y. Lv, Z. Zeng, *Colloid Surface A* 2013, **422**, 90.
37. Y. Tang, G. Zhang, C. Liu, S. Luo, X. Xu, L. Chen, B. Wang, *J. Hazard. Mater.* 2013, **252-253**, 115.
38. Y. Lin, Z. Geng, H. Cai, L. Ma, J. Chen, J. Zeng, N. Pan, X. Wang, *Eur. J. Inorg. Chem.* 2012, 4439.
39. S. Linley, Y. Y. Liu, C. J. Ptacek, D. W. Blowes, F. X. Gu, *ACS Appl. Mater. Interfaces* 2014, **6**, 4658.
40. J. S. Lee, K. H. You, C. B. Park, *Adv. Mater.* 2012, **24**, 1084.